Appl Biochem Biotechnol (2010) 162:1080–1094
DOI 10.1007/s12010-009-8903-6

Potential of Xanthones from Tropical Fruit Mangosteen as Anti-cancer Agents: Caspase-Dependent Apoptosis Induction In Vitro and in Mice

Ramida Watanapokasin · Faongchat Jarinthanan · Alan Jerusalmi · Sunit Suksamrarn · Yukio Nakamura · Supawadee Sukseree · Wanlaya Uthaisang-Tanethpongtamb · Piniti Ratananukul · Takeshi Sano

Received: 16 August 2009 / Accepted: 28 December 2009 /
Published online: 26 January 2010

Abstract The pericarp of mangosteen (*Garcinia mangostana* L.) is rich in various xanthones that are known to possess unique biological activities. In this work, we characterized the anti-proliferative and cytotoxic activities of mangosteen xanthones both in vitro and in mice. In vitro analysis with a human colorectal adenocarcinoma cell line, COLO 205, showed that mangosteen xanthones not only inhibit the proliferation of target cells but also induce their death by apoptosis that involves the activation of the caspase cascade. In vivo analysis using a mouse subcutaneous tumor model with COLO 205 cells showed that, at relatively low doses, the growth of tumors was repressed upon intratumoral administration of mangosteen xanthones. When a higher dose of mangosteen xanthones was administered, the size of tumors was reduced gradually, and, in some mice, the disappearance of tumors was seen. Histopathological evaluation and biochemical analysis of tumors that received mangosteen xanthones indicate the induction of apoptosis in tumors, which resulted in the repression of their growth and the reduction of their sizes. These results demonstrate the potential of mangosteen xanthones to serve as anti-cancer agents for the chemotherapy of cancer.

Keywords *Garcinia mangostana* L (mangosteen) · Apoptosis · Caspase · Mangostin · Cancer chemotherapy

R. Watanapokasin (✉) · F. Jarinthanan · S. Sukseree · W. Uthaisang-Tanethpongtamb
Department of Biochemistry, Faculty of Medicine, Srinakharinwirot University, Bangkok, Thailand
e-mail: ramidawa@yahoo.com
e-mail: yuwadee@swu.ac.th

A. Jerusalmi · T. Sano
Center for Molecular Imaging Diagnosis and Therapy and Basic Science Laboratory, Department of Radiology, Beth Israel Deaconess Medical Center, Harvard Medical School, Boston, MA 02215, USA

S. Suksamrarn · P. Ratananukul
Department of Chemistry, Faculty of Science, Srinakharinwirot University, Bangkok, Thailand

Y. Nakamura
Howard Hughes Medical Institute, Department of Orthopedic Surgery, Children's Hospital, Boston, MA 02115, USA

Introduction

A variety of tropical plants have useful biological activities, some of which offer potential therapeutic applications. A tropical evergreen tree, mangosteen (*Garcinia mangostana* L.) in the Clusuaceae family, has been used in Southeast Asia as indigenous medicine for skin infection, diarrhea, chronic ulcer, and wounds [1]. Phytochemical studies showed that the pericarp of mangosteen is rich in a variety of oxygenated and prenylated xanthones [2, 3], including α- and γ-mangostins, and that these xanthones possess unique biological properties, such as anti-mycobacterial [4], anti-fungal [5], anti-oxidant [6–9], anti-inflammatory [10, 11], and cytotoxic activities [12–17]. For example, a primary xanthone in the pericarp of mangosteen, α-mangostin, has been shown to induce mitochondrial dysfunction in the human acute promyelocytic leukemia cell line HL-60 [13]. Several xanthone derivatives, extracted from the stem and root bark of mangosteen, particularly α-mangostin, mangostanol, and garcinone D, showed strong cytotoxic activity against a human T-lymphoblastoid cell line [18]. Garcinone E also showed potent cytotoxicity against several hepatocellular carcinoma cell lines [12]. In addition, an ethanolic extract of the pericarp of mangosteen, which contains mangostins, exhibited anti-proliferative activity against a human mammary gland adenocarcinoma cell line, SK-BR-3 [14]. Crude α-mangostin showed potent chemopreventive effect on colon preneoplastic lesions induced by 1,2-dimethylhydrazine in rats [19]. The new prenylated xanthones were isolated from young fruits of *G. mangostana* L. showed cytotoxic activity against epidermoid carcinoma of the mouth (KB), breast cancer (BC-1), and small cell lung cancer (NCI-H187) [17]. These and other studies suggest that xanthones and their derivatives from the pericarp of mangosteen could be useful as chemotherapeutic agents for the treatment of certain cancers.

The objective of the present study was to characterize the anti-proliferative and cytotoxic activities of xanthones, which were extracted from the pericarp of mangosteen [termed "mangosteen xanthones (MX)"]. In particular, we were interested in the potential of MX to serve as an anti-cancer agent. Initially, the anti-proliferative and cytotoxic activities of MX were investigated in vitro by using several human colorectal cancer cell lines. Then, a mouse subcutaneous tumor model, prepared by using athymic nude mice with a human colorectal adenocarcinoma cell line, was used to determine the abilities of MX to repress the growth of tumors and to kill target tumor cells under in vivo conditions.

Materials and Methods

Mangosteen Xanthones

The fruit of mangosteen (*G. mangostana*) was harvested from the Kombang District, Chantaburi Province, Thailand in 2007. A voucher specimen is deposited at the Faculty of Science, Ramkhamhaeng University, Thailand (Porntip Wongnapa No. 002) and was identified by Nopporn Damrongsiri. The pericarp of mangosteen was collected, air-dried, and pulverized. Xanthones were extracted from pulverized pericarps by thorough extraction with ethyl acetate at 50°C. The extract was dried in vacuo, and the resulting yellowish powder was used as MX. MX was analyzed at ambient temperature by high-performance liquid chromatography (HPLC) using an analytical Synergi reversed-phase column (150× 4.6 mm, 4 μm; Phenomenex, CA) with a C_{18} guard column (4.0×2.0 mm). MX in a total injection volume of 50 μl was applied to the column, and elution was done at a flow rate of

0.5 ml/min by using mobile phases containing acetonitrile (component A), 2% (*v*/*v*) acetic acid in water (B), and *n*-butanol (C) with the following gradient profiles: A:B:C from 30:70:0 to 45:45:10 in 2 min; from 45:45:10 to 80:15:5 in 23 min, from 80:15:5 to 80:20:0 in 2 min, from 80:20:0 to 95:5:0 in 8 min, and isocratic at 95:5:0 for 25 min. Eluted xanthones were detected by absorbance at 254 nm.

Cell Lines

The following four human colorectal cancer cell lines were used: COLO 205 (colorectal adenocarcinoma), CX-1 (colonic carcinoma), MIP-101 (colorectal carcinoma), and SW620 (colorectal adenocarcinoma). COLO 205 and SW620 were obtained from the American Type Culture Collection (Manassas, VA, USA). CX-1 and MIP-101 were generous gifts from Peter Thomas, Boston University School of Medicine, Boston, MA, USA. COLO 205 and MIP-101 were maintained in the RPMI 1640 medium (Invitrogen), supplemented with 10% fetal calf serum (Invitrogen). CX-1 and SW620 were cultured in Dulbecco's modified Eagle's medium (Invitrogen), supplemented with 10% fetal calf serum.

Cell Proliferation and Cell Viability Assays

The cytotoxic activity of MX was initially determined by cell proliferation analysis using standard 3-(4,5-dimethylthiazol-2-yl)-2,5-diphenyltetrazolium bromide (MTT) assays [20, 21]. Target cells were cultured in flat-bottom 96-well plates at 37°C for 24 h (initial number of cells, 2×10^4 per well). MX, dissolved in dimethyl sulfoxide (DMSO), was added to culture wells at varying concentrations, and cells were incubated at 37°C for 24 h. The final DMSO concentration in each well was 0.05%, at which concentration no appreciable effect on cell proliferation was seen. Then, 100 μl of 5.0 mg/ml MTT in culture media was added to each well, which was incubated at 37°C for 2 h. After culture media were removed, formazan, the metabolic product of MTT, in each well was dissolved in DMSO, and the absorbance at 595 nm was determined.

Effect of MX on the viability of COLO 205 cells was analyzed by using a trypan blue exclusion method. Target cells were cultured in flat-bottom 96-well plates at 37°C for 24 h (initial number of cells, 2×10^4 per well). MX, dissolved in DMSO, was added to culture wells at varying concentrations (0–40 μg/ml), and cells were incubated at 37°C. Cells were collected periodically and mixed with trypan blue. Then, the number of viable cells was determined with hemocytometers under a light microscope. Cell viability is expressed as a percentage of the number of viable cells to that of the control, to which DMSO without MX was applied.

Microscopic Analysis of Cell and Nucleus Morphology

COLO 205 cells were cultured in 24-well culture plates at the initial number of cells, 2×10^4 per well for 3 and 6 h in the presence of 20 μg/ml α-mangostin. As controls, cells were cultured in the same manner in the absence of α-mangostin. After culture media were removed, cells were washed once with phosphate-buffered saline (PBS) and examined for their morphology under a phase-contrast inverted microscope (model CKX31/CKX41, Olympus).

When the morphology of cell nuclei was analyzed, COLO 205 cells were initially grown in six-well culture plates at the cell density at 2×10^6 per well for 24 h. Then, α-mangostin was added to each well to a final concentration of 20 μg/ml for 3 and 6 h. Control cells

were grown in the absence of α-mangostin. Cells were collected by trypsinization and fixed with methanol. Then, cell nuclei were stained with 1 μg/ml Hoesch 3443 (Sigma) at 37°C for 15 min in the dark. Stained cells were examined under a fluorescence inverted microscope (model BX50, Olympus) with an appropriate filter.

Analysis of DNA Fragmentation

Fragmentation of chromosomal DNA was analyzed by using standard agarose gel electrophoresis. COLO 205 cells were cultured in the presence of varying concentrations of MX (0–40 μg/ml) at 37°C for 6 h. Cells were gently detached from culture wells and collected by centrifugation. The resulting cell pellets were incubated at 4°C for 24 h in 500 μl of a lysis solution, consisting of 5 mM Tris–Cl (pH 8.0), 0.5% Triton X-100, and 20 mM EDTA. DNA fractions were extracted from the cell lysates with phenol-chloroform-isoamyl alcohol and electrophoresed on 1.8% agarose gels. DNA was stained with ethidium bromide and visualized under a UV transilluminator.

Western Blot Analysis of Caspase-3 and Caspase-8

Activation of caspase-3 and caspase-8 was analyzed by Western blot analysis. COLO 205 cells were cultured in six-well culture plates at 4×10^6 cells per well and then treated with varying concentrations of MX (0–50 μg/ml) for 3 h. Cells were washed with PBS and lysed using a lysis solution containing 1% SDS, 50 mM Tris–Cl (pH 8.0), and 1 mM DTT. The resulting solutions were subjected to SDS-PAGE using 12% polyacrylamide gels (Ready Gels, Bio-Rad), and proteins were transferred onto Immobilon P membrane (Millipore). The resulting blots were subjected to immuno-detection of caspase-3 or caspase-8. For immuno-detection of caspase-3, a rabbit polyclonal antibody against human caspase-3 (8G10; Cell Signaling Technology) and a goat anti-rabbit IgG, conjugated to horse radish peroxidase (Cell Signaling Technology), were used as the primary and secondary antibodies, respectively. Similarly, a mouse polyclonal antibody against human caspase-8 (1C12; Cell Signaling Technology) and a goat anti-mouse IgG, conjugated to horse radish peroxidase (Cell Signaling Technology), were used for the immuno-detection of caspase-8. The peroxidase activity of bound secondary antibodies on the blots was detected by using an ECL Plus Western Blotting Detection System (Amersham Biosciences). The same blots were also used for immuno-detection of actin using a rabbit polyclonal antibody against human β-actin (Cell Signaling Technology) to estimate the amount of cell components in each lane.

Analysis of Caspase-3 Activity

Caspase-3 activity was determined by a fluorometric assay. COLO 205 cells were cultured in six-well culture plates (2×10^6 cells per well) and then pre-incubated at 37°C for 1 h with a peptide inhibitor of caspase-3, caspase-8, or caspase-9 (Z-DEVD-FMK, Z-IETD-FMK, or Z-LEHD-FMK, respectively; Calbiochem). Cells were then treated with 30 μg/ml MX at 37°C for 3 h and washed twice with ice-cold PBS. Washed cells were incubated for 10 min on ice with occasional mixing in 50 μl of a lysis solution, consisting of 100 mM NaCl, 50 mM HEPES (pH 7.4), 0.1% CHAPS, 1 mM DTT, and 100 μM EDTA. The resulting cell lysates were centrifuged at 4°C at 1,000×*g* for 5 min, and the supernatants were used to determine the activity of caspase-3 using a fluorometric caspase-3 activity assay kit (Calbiochem).

Western Blot Analysis of the Release of Cytochrome c

Release of cytochrome c from mitochondria was determined by Western blot analysis as described previously [22]. COLO 205 cells were cultured in six-well culture plates (4×10^6 cells per well) and then incubated in the presence of 30 μg/ml MX for 0–9 h. Cells were washed with PBS and re-suspended in an ice-cold S-100 homogenization solution, consisting of 0.3 M sucrose, 10 mM KCl, 1.5 mM $MgCl_2$, 1 mM EDTA, 1 mM DTT, and 20 mM HEPES (pH 7.5), with a mixture of protease inhibitors (1 mM PMSF, 10 μM aprotinin, 10 μM leupeptin, and 10 μM pepstatin A). Cell suspensions were sonicated for 10 s to lyse the cells, followed by the removal of unlysed cells and nuclei by centrifugation at 4°C at 500×*g* for 5 min. The resulting cell lysates was further centrifuged at 4°C at 10,000×*g* for 30 min. The supernatants (cytosol fractions) were separated by SDS-PAGE using 12% polyacrylamide gels (Ready Gels, Bio-Rad), and proteins were transferred onto Immobilon P membrane (Millipore). The resulting blots were subjected to immuno-detection of cytochrome c, which had been released from mitochondria, using a mouse monoclonal antibody against human cytochrome c (clone 7H8, Santa Cruz, Biotechnology) with goat anti-mouse IgG, conjugates to horse radish peroxidase (Cell Signaling Technology), as secondary antibody. The peroxidase activity of bound secondary antibodies on the blots was detected by using an ECL Plus Western Blotting Detection System (Amersham Biosciences). As in the Western blot analysis of caspase-3 above, the same blots were also used for immuno-detection of β-actin using a rabbit polyclonal antibody against human β-actin (Cell Signaling Technology) to estimate the amount of cell components in each lane.

In Vivo Evaluation of the Effect of MX Using a Mouse Subcutaneous Tumor Model

All animal procedures were carried out in accordance with NIH guidelines (#85-23). A mouse subcutaneous tumor model was prepared by using athymic nude mice ($NCr^{nu/nu}$, male, 6–8 weeks old, 22–24 g; Taconic) with the cell line COLO 205. Cultured COLO 205 cells were injected percutaneously into the right flank of each mouse (5×10^6 cells per tumor). The growth of tumors was monitored by the measurement of their dimensions using calipers, and their volumes were calculated by using the following equation: $\text{Volume} = (\text{width})^2 \times \text{length} \times 0.52$. When the volumes of tumors reached 70–100 mm^3, mice were randomized, and varying amounts of MX (0.024–3.0 mg per tumor), dissolved in 50 μl of 80% DMSO in PBS, were administered intratumorally. Control mice received 50 μl of 80% DMSO in PBS without MX. The tumor sizes were monitored periodically up to day 27 post-administration of MX (or 80% DMSO in PBS for control mice).

On days 10 and 20 post-administration, several mice in two groups, which received 80% DMSO in PBS without MX (control) or with 3.0 mg MX, were euthanized, and their tumors were collected. Collected tumor samples were fixed in 4% paraformaldehyde in PBS, embedded in paraffin, and sectioned at 7 μm. The resulting tumor sections were stained with hematoxylin and eosin and subjected to histopathological evaluation by an experienced pathologist at the Rodent Histopathology Core of the Dana-Farber/Harvard Cancer Institute.

Tumor samples, which were collected on day 10 post-administration above, were also analyzed for the activation of caspase-3 by Western blot analysis. Collected tumor samples were dissolved in a lysis solution containing 1% SDS, 50 mM Tris–Cl (pH 8.0), and 1 mM DTT. The resulting solution was subjected to Western blot analysis for caspase-3 or caspase-8 using a rabbit polyclonal antibody against human caspase-3 (8G10; Cell

Signaling Technology) or a mouse polyclonal antibody against caspase-8 (1C12; Cell Signaling Technology), respectively, following SDS-PAGE and transfer of proteins onto Immobilon P membrane (Millipore), as described above for cultured COLO 205 cells.

Statistical Analysis

Data are presented as means ± SD. Statistical comparisons were performed by using two-tailed Student's *t* tests and two-way ANOVA at a 95% confidence interval ($p<0.05$).

Results and Discussion

In the present study, we have characterized the anti-proliferative and cytotoxic activities of xanthones, purified from the pericarp of mangosteen, with the following two primary focuses. One was to find a clue to the mechanism(s), by which these xanthones exert anti-proliferative and cytotoxic activities on target tumor cells. The other was to ask whether or not they can also show the anti-proliferative and cytotoxic activities against target tumors under in vivo conditions. We used MX, which is a mixture of xanthones with α-mangostin as a major component.

Preparation and HPLC Analysis of MX

MX was extracted from the pericarp of mangosteen, as described in "Materials and Methods". HPLC analysis of MX was performed by using a reversed-phase column to determine the concentrations of primary magostins (Fig. 1). By using purified materials as standards, the concentrations of two primary mangostins, α- and γ-mangostins, in MX were estimated at 48.04 and 6.40 mg/g, respectively. Our routine chromatographic isolation and purification of the ethyl acetate extract obtained from the dried pericarp of mangosteen revealed that α- and γ-mangostins were usually the two major xanthones obtained. Other xanthones, epicatechin, and beta-sitosterol were isolated in very small amount. None of other components including anthocyanin was detected. Moreover, our unpublished 3D HPLC chromatogram analysis on the same extract was consistent with the isolation result.

Effect of MX on the Growth of Human Colonic Cancer Cell Lines

Initially, the anti-proliferative activity of MX against target cells was analyzed in vitro by using MTT assays [18, 19]. We used the following four human colonic cancer cell lines as targets: COLO 205, CX-1, MIP-101, and SW620. The proliferation of all of the four cell lines was inhibited by the addition of MX to culture media (data not shown). The half maximal inhibitory concentration (IC_{50}) of MX for each cell line was determined from three independent sets of experiments, in which target cells were treated with varying concentrations of MX: COLO 205, 7.50±0.54 μg/ml; CX-1, 17.7±1.15 μg/ml; MIP-101, 10.0±0.52 μg/ml; and SW620, 16.1±0.86 μg/ml. Among the four cell lines tested, the highest anti-proliferation effect of MX was seen on COLO 205 cells. Thus, we used this cell line as the primary target in subsequent experiments.

Effect of MX on the viability of COLO 205 cells was analyzed by using a trypan blue exclusion method (Fig. 2). As expected, the viability of COLO 205 cells decreased by the treatment with MX in both concentration- and time-dependent manners. Treatment of COLO 205 cells with MX at 30 μg/ml or higher for 12 h reduced the number of viable cells

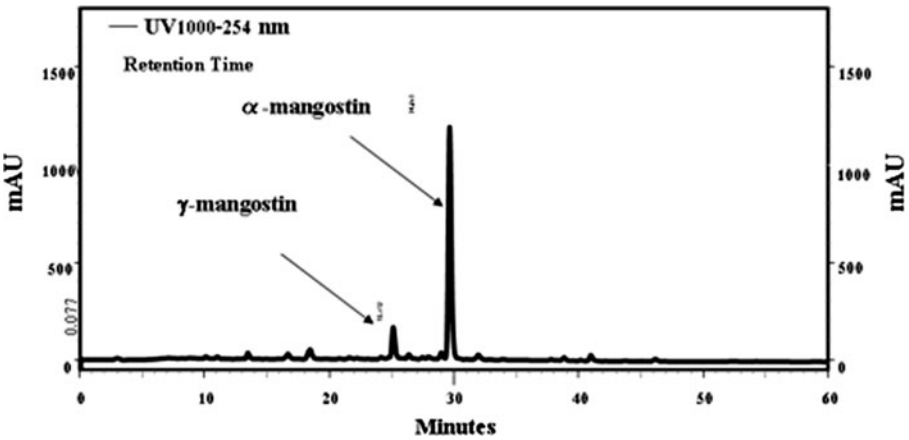

Fig. 1 HPLC analysis of MX. Two major mangostins, α- and γ-mangostins, which had retention times of 29.6 and 25.1 min, respectively, in MX were quantitated by using purified materials as standards. The identify of these mangostins was also confirmed by spectral analysis

to approximately 10% of the control, in which target cells were grown in the absence of MX. The results of these cell proliferation and viability assays suggest that MX not only inhibits the proliferation of COLO 205 cells but it also induces their death.

Changes in the Morphology of Target Cells and Their Nuclei upon Treatment with MX

One potential mechanism of the death of target cells upon treatment with MX, shown in Fig. 2, is the induction of apoptosis. To test this, the changes in the cell morphology upon treatment with MX were investigated (Fig. 3; left images). Inverted microscopic images of COLO 205 cells after treatment with 30 μg/ml MX for 3 and 6 h (B and C, respectively) show considerable cell rounding and blebbing, as well as the presence of apoptotic bodies.

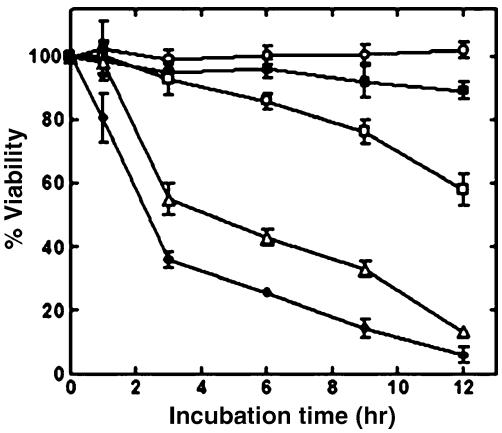

Fig. 2 Effect of MX on the viability of COLO 205 cells. COLO 205 cells were cultured in the presence of varying concentrations of MX (0–40 μg/ml) and collected periodically (0–12 h), for viability assay using a trypan blue exclusion method. Cell viability is expressed as a percentage of the number of viable cells to that of the control, which was grown in the absence of MX. Each data point shown is the mean ± SD from three independent experiments

In particular, at 6 h (C), a large amount of cells detached from culture plates, and only cell debris remained. Such morphological changes were not seen with control cells (A), which were cultured in the absence of MX.

Cells were also subjected to the staining of cell nuclei with HOESCH 3443, and stained cells were examined under a fluorescence microscope (Fig. 3; right images). Chromatin condensation and fragmentation, characteristic of the nucleus of apoptotic cells, were seen with COLO 205 cells, which had been treated with 30 μg/ml MX for 3 and 6 h (B and C, respectively), while the nuclei of control cells without MX treatment (A) showed normal morphology. These results suggest that the proliferation inhibition and the death of target cells upon treatment with MX are caused by the induction of apoptosis.

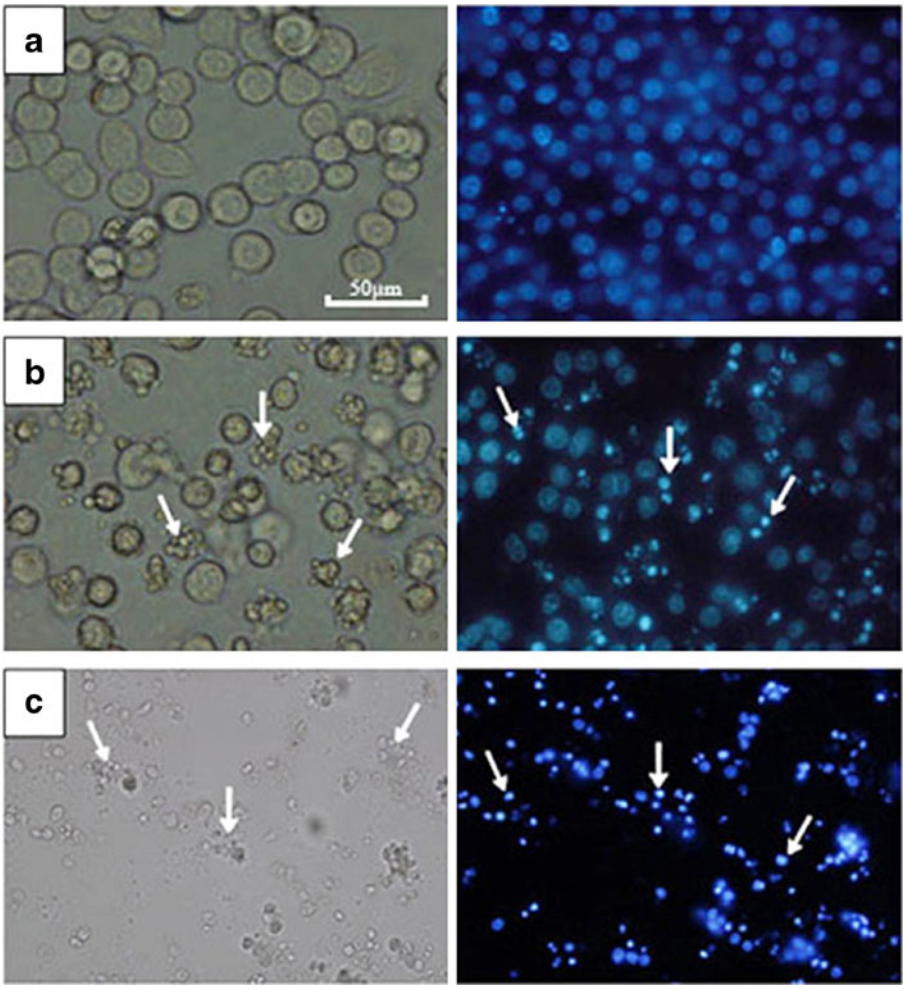

Fig. 3 Effect of MX on the morphology of COLO 205 cells and their nuclei. COLO 205 cells were cultured for 3 and 6 h in presence of 30 μg/ml MX. As controls, cells were cultured in the same manner in the absence of MX. Cell morphology was determined under a phase-contrast inverted microscope (*left images*). The nuclear condensation was detected by HOESCH 3443 staining (*right images*). **a** Control (without MX), **b** 3 h, **c** 6 h

Fragmentation of Chromosomal DNA in Target Cells upon Treatment with MX

Fragmentation of chromosomal DNA, which generally occurs in apoptotic cells prior to the disintegration of cell membrane, was analyzed for COLO 205 cells upon treatment with MX. COLO 205 cells were treated with varying concentrations of MX (0–40 μg/ml) for 6 h, followed by the extraction of DNA. Extracted DNA samples were analyzed by agarose gel electrophoresis (Fig. 4). Fragmentation of chromosomal DNA was apparent by the presence of DNA ladders when COLO 205 cells were treated with MX at 20 μg/ml or higher. This result supports the notion above that MX treatment induces apoptosis in COLO 205 cells.

Activation of Caspase-3 and Caspase-8 in Target Cells upon Treatment with MX

To further investigate the induction of apoptosis by MX treatment, the activation of caspase-3 and caspase-8, a primary effector caspase and an initiator caspase, respectively, was analyzed by Western blotting (Fig. 5a and b). COLO 205 cells were treated with varying concentrations of MX (0–50 μg/ml) for 3 h. Cells were lysed, and the resulting cell lysates were subjected to SDS-PAGE, followed by Western blot analysis, in which caspase-3 and caspase-8 were detected by using polyclonal antibodies against caspase-3 and caspase-8, respectively. The amount of the pro-enzyme form of caspase-3 (pro-caspase-3;

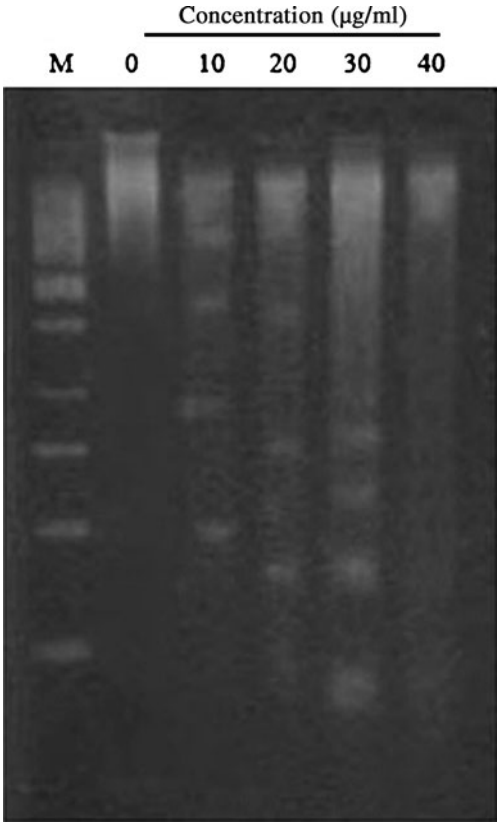

Fig. 4 Fragmentation of chromosomal DNA in COLO 205 cells upon treatment with MX. COLO 205 cells were treated with varying concentrations of MX (0–40 μg/ml) for 6 h. Extracted DNA fractions were electrophoresed on 1.8% agarose gels and stained with ethidium bromide

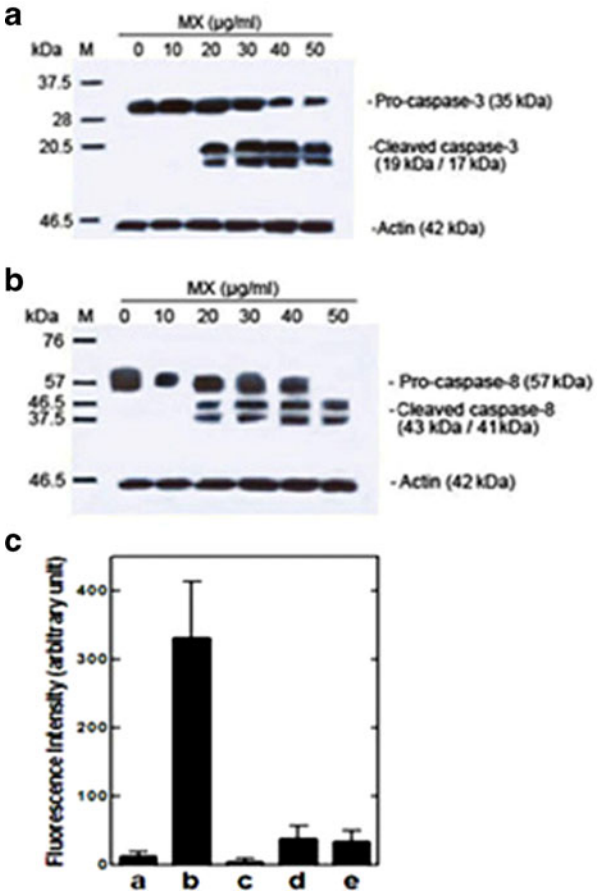

Fig. 5 Activation of caspase-3 and caspase-8 in COLO 205 cells upon treatment of MX. **a** and **b** COLO 205 cells were treated with varying concentrations of MX (0–50 μg/ml) for 3 h and subjected to Western blot analysis for caspase-3 and caspase-8 detection. **c** Caspase-3 activity was assayed after treatment of the cells with inhibitor of caspase-3, caspase-8, or caspase-9, respectively, followed by 30 μg/ml of MX. *a* Control (without MX), *b* after MX treatment, *c* pre-incubation with caspase-3 inhibitor, *d* pre-incubation with caspase-8 inhibitor, *e* pre-incubation with caspase-9 inhibitor

35 kDa) and pro-caspase-8 (57 kDa) decreased with increasing the concentration of MX. Accordingly, cleaved, activated forms of caspase-3 (17 and 19 kDa) and caspase-8 (41 and 43 kDa) became apparent upon treatment of MX at 20 μg/ml or higher. No apparent cleavage of pro-caspase-3 or caspase-8 is seen with control cells, which were cultured in the absence of MX. This result reveals that the treatment of COLO 205 cells with MX induces the activation of both caspase-3 and caspase-8.

Activation of caspase-3 and caspase-8 in COLO 205 cells upon treatment with MX was further investigated by activity assays (Fig. 5c). Low caspase-3 activity was seen with control cells, which were cultured in the absence of MX (a). In contrast, COLO 205 cells, which had been treated with MX at 30 μg/ml for 3 h, showed much higher caspase-3 activity ($p<0.05$; b). Pre-incubation of target cells with a peptide inhibitor of caspase-3, prior to the addition of MX, effectively inhibited the activation of caspase-3, as expected (c). In addition, pre-incubation of target cells with a peptide inhibitor of caspase-8 or

caspase-9, each of which is known to activate caspase-3, greatly inhibited the activation of caspase-3 by MX treatment (d and e).

These results indicate that treatment of COLO 205 cells with MX triggers the activation of the caspase cascade of the apoptosis process. Since caspase-8 and caspase-9 are involved primarily in the extrinsic (or receptor-mediated) and intrinsic (or mitochondrial) pathways, respectively, of apoptosis, the induction of apoptosis in target cells by MX may be associated with the activation of both pathways.

Release of Cytochrome c from the Mitochondria in Target Cells upon Treatment with MX

Release of cytochrome c from the mitochondria, which is involved in the intrinsic (mitochondrial) pathway of apoptosis, was analyzed for COLO 205 cells that had been treated with MX (Fig. 6). No appreciable amount of cytochrome c was detected in the cytosol fraction of control COLO 205 cells prior to the addition of MX (time 0). In contrast, treatment of COLO 205 cells with MX at 30 μg/ml for 3, 6, and 9 h resulted in the release of cytochrome c to the cytosol. The amount of released cytochrome c appears to become greater with increasing the incubation time. This result confirms the activation of the intrinsic pathway of apoptosis by MX treatment.

Effect of MX on the Growth of Tumors in Mice

The results of a series of in vitro experiments, described above, suggest that MX treatment results in the death of target cells by the induction of apoptosis. These results prompted us to investigate if MX could also induce apoptosis of target cells under in vivo conditions.

A mouse subcutaneous tumor model was prepared by using athymic nude mice ($NCr^{nu/nu}$; Taconic) with COLO 205 cells. When the volume of each tumor reached 70–100 mm^3, varying amounts of MX (0.024–3.0 mg), dissolved in 50 μl of 80% DMSO in PBS, were administered intratumorally, and the volumes of tumors were monitored (Fig. 7). Control mice received 50 μl of 80% DMSO in PBS without MX intratumorally. When relatively low doses of MX (0.024, 0.12, and 0.6 mg per tumor) were used, the growth of tumors was initially repressed for approximately 10 days after administration of MX. However, the re-growth of the tumors was seen thereafter, and the re-growth rate appeared to be dependent on the dose of MX used; i.e., the lower the dose of MX was, the greater the re-growth rate became. In contrast, when MX was used at a dose of 3.0 mg per

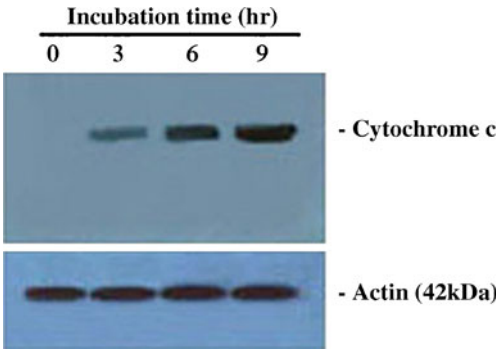

Fig. 6 Release of cytochrome c from the mitochondria in COLO 205 cells upon treatment with MX. COLO 205 cells were treated with 30 μg/ml MX for 0–9 h. Cytosol fractions were separated by SDS-PAGE and subjected to immuno-detection of cytochrome c

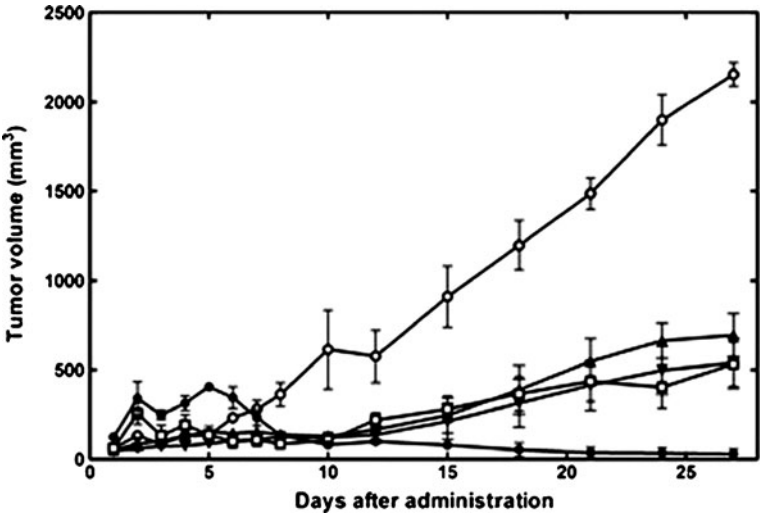

Fig. 7 Effect of MX on the growth of tumors in a mouse subcutaneous tumor model. When the volumes of tumors reached 70–100 mm^3, varying amounts of MX (0.024–3.0 mg per tumor) were administered intratumorally. Control mice received no MX. The volume of each tumor was monitored periodically up to day 27 post-administration. *unfilled circle* Control (without MX), *filled triangle* 0.024 mg MX, *filled inverted triangle* 0.12 mg MX, *unfilled square* 0.6 mg MK, *filled circle* 3.0 mg MX

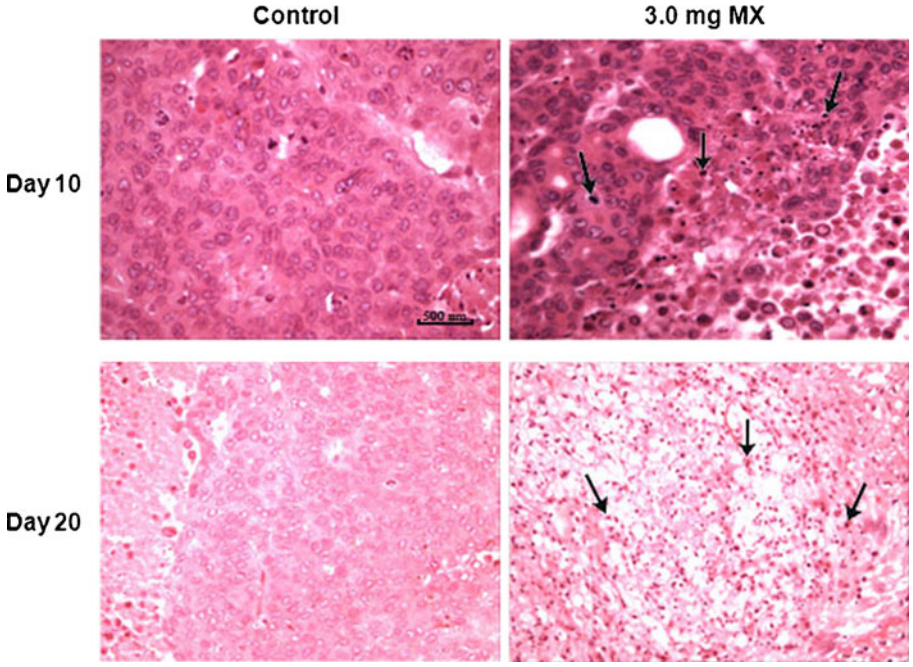

Fig. 8 Histopathological analysis of tumors upon intratumoral administration of MX. On days 10 and 20 post-administration of MX into a mouse subcutaneous tumor model, described in Fig. 7 above, several mice were euthanized. Collected tumor samples were fixed, embedded in paraffin, and sectioned. The resulting tumor sections were stained with hematoxylin and eosin and subjected to histopathological evaluation

tumor, the reduction of tumor volumes was seen from around day 5 post-administration and continued. No apparent re-growth of tumors was seen until mice were euthanized on day 27 post-administration. In some mice, tumors appeared to have disappeared on around day 20 post-administration.

Tumors were collected from mice that received 3.0 mg MX per tumor on days 10 and 20 post-administration, followed by the preparation of tumor sections that were then stained with hematoxylin and eosin. Tumor sections with hematoxylin/eosin staining were also prepared from control mice, which received the solvent alone (80% DMSO in PBS) without MX. These stained tumor sections were subjected to histopathological evaluation (Fig. 8). Tumor sections, derived from control mice, showed normal cellularity with intact nuclei. In contrast, tumor sections, which were prepared on day 10 post-administration from mice that had received 3.0 mg MX, show a large number of apoptotic cells with chromatin condensation (pyknosis) and nuclear fragmentation (karyorrhexis), along with the formation of apoptotic bodies. Very poor cellularity is seen in tumor sections on day 20 post-administration, suggesting that the majority of cells had undergone apoptosis.

Tumor samples from the two groups of mice that were collected on day 10 post-administration were also subjected to Western blot analysis for the activation of caspase-3 and caspase-8 (Fig. 9a and b). Tumor samples from control mice showed no appreciable

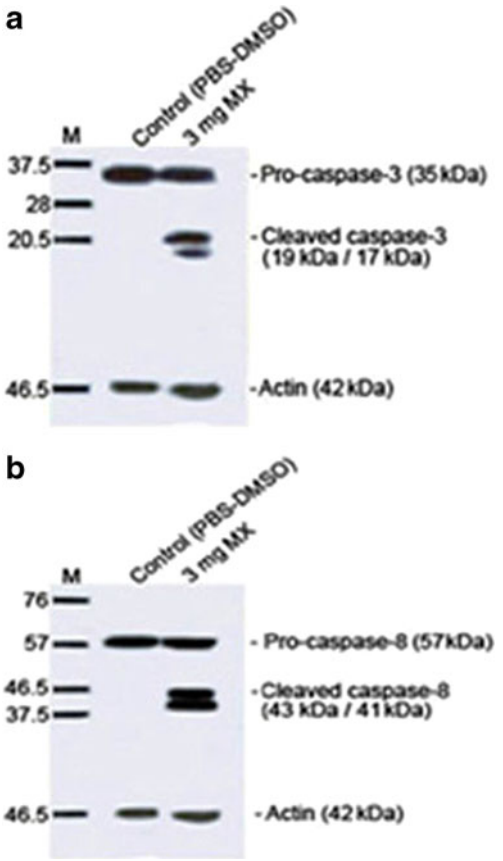

Fig. 9 Western blot analysis of the activation of caspase-3 and caspase-8 upon intratumoral administration of MX. **a** and **b** Tumor samples, which were collected on day 10 post-administration as described in Fig. 7 above, were also analyzed for the activation of caspase-3 or caspase-8 by Western blot analysis

amounts of cleaved, activated forms of caspase-3 (17 and 19 kDa) and caspase-8 (41 and 43 kDa). In contrast, activated forms of caspase-3 and caspase-8 were seen in tumors, which had received 3.0 mg MX. This result reveals the activation of the caspase cascade of the apoptosis process in target tumors upon intratumoral administration of MX, as seen in vitro with the application of MX to target cells (Fig. 5a and b).

These results indicate that MX can actively kill tumor cells in vivo in tumor-bearing mice, rather than merely repress their growth, resulting in the regression of target tumors. They also suggest that the death of target tumor cells upon administration of MX is caused by the induction of apoptosis that involves the activation of the caspase cascade.

In conclusion, MX can efficiently induce apoptosis in target tumor cells, COLO 205, both in vitro and in vivo in a dose-dependent manner. Induction of apoptosis by MX appears to involve both the intrinsic and extrinsic pathways of apoptosis, resulting in the activation of the caspase cascade. These results suggest the great potential for MX to serve as an effective anti-cancer agent for the chemotherapy of cancer.

Acknowledgments This work was supported, in part, by the National Research Council of Thailand, Faculty of Medicine and Center for the Development of Value-added Natural Products Srinakharinwirot University. R.W. was supported by the Fulbright Visiting Scholar Program 2006–2007, the Thailand–United States Education Foundation (Fulbright).

References

1. Mahabusarakam, W., Iriyachitra, P., & Taylor, W. C. (1987). *Journal of Natural Products, 50*, 474–478.
2. Peres, V., & Nagem, T. J. (1997). *Phytochemistry, 44*, 191–214.
3. Peres, V., Nagem, T. J., & de Oliveira, F. F. (2000). *Phytochemistry, 55*, 683–710.
4. Suksamrarn, S., Suwannapoch, N., Phakhodee, W., Thanuhiranlert, J., Ratananukul, P., Chimnoi, N., et al. (2003). *Chemical and Pharmaceutical Bulletin (Tokyo), 51*, 857–859.
5. Gopalakrishnan, G., Banumathi, B., & Suresh, G. (1997). *Journal of Natural Products, 60*, 519–524.
6. Jung, H. A., Su, B. N., Keller, W. J., Mehta, R. G., & Kinghorn, A. D. (2006). *Journal of Agricultural and Food Chemistry, 54*, 2077–2082.
7. Mahabusarakam, W., Proudfoot, J., Taylor, W., & Croft, K. (2000). *Free Radical Research, 33*, 643–659.
8. Williams, P., Ongsakul, M., Proudfoot, J., Croft, K., & Beilin, L. (1995). *Free Radical Research, 23*, 175–184.
9. Yoshikawa, M., Hardy, E., Miki, A., Tsukamoto, K., Liang, S., Yamahara, J., et al. (1994). *Journal of the Pharmacy Society of Japan, 114*, 129–133.
10. Chen, L. G., Yang, L. L., & Wang, C. C. (2008). *Food and Chemical Toxicology, 46*, 688–693.
11. Nakatani, K., Nakahata, N., Arakawa, T., Yasuda, H., & Ohizumi, Y. (2002). *Biochemical Pharmacology, 63*, 73–79.
12. Ho, C. K., Huang, Y. L., & Chen, C. C. (2002). *Planta Medica, 68*, 975–979.
13. Matsumoto, K., Akao, Y., Ohguchi, K., Ito, T., Tanaka, T., Iinuma, M., et al. (2005). *Bioorganic & Medicinal Chemistry, 13*, 6064–6069.
14. Moongkarndi, P., Kosem, N., Luanratana, O., Jongsomboonkusol, S., & Pongpan, N. (2004). *Fitoterapia, 75*, 375–377.
15. Nakagawa, Y., Iinuma, M., Naoe, T., Nozawa, Y., & Akao, Y. (2007). *Bioorganic & Medicinal Chemistry, 15*, 5620–5628.
16. Sato, A., Fujiwara, H., Oku, H., Ishiguro, K., & Ohizumi, Y. (2004). *Journal of Pharmacological Science, 95*, 33–40.
17. Suksamrarn, S., Komutiban, O., Ratananukul, P., Chimnoi, N., Lartpornmatulee, N., & Suksamrarn, A. (2006). *Chemical and Pharmaceutical Bulletin (Tokyo), 54*, 301–305.

18. Ee, G. C., Daud, S., Izzaddin, S. A., & Rahmani, M. (2008). *Journal of Asian Natural Products Research, 10*, 475–479.
19. Nabandith, V., Suzui, M., Morioka, T., Kaneshiro, T., Kinjo, T., Matsumoto, K., et al. (2004). *Asian Pacific Journal of Cancer Prevention, 5*, 433–448.
20. Mosmann, T. (1983). *Journal of Immunological Methods, 65*, 55–63.
21. Uthaisang, W., Reutrakul, V., Krachangchaeng, C., Wilairat, P., & Fadeel, B. (2004). *Cancer Letters, 208*, 171–178.
22. Arnoult, D., Parone, P., Martinou, J. C., Antonsson, B., Estaquier, J., & Ameisen, J. C. (2002). *Journal of Cell Biology, 159*, 923–929.